A Survey of Many Body Hadrondynamics. I

A. GIOVANNINI and E. PREDAZZI

Istituto di Fisica dell'Università, Torino
und
Istituto Nazionale di Fisica Nucleare, Sezione di Torino

Recebido em 19 de Fevereiro de 1971

Contents

1. Introduction*

The interest in hadronic collisions with final states of high multiplicity ($n \gg 2$ if n is the number of particles of the final state), is not new but has received an increasing attention in recent years. This is evident from a glance at the prominence given to this subject in international meetings and from the general activity in the field.

The reasons for such an interest lies, first of all, in the experimental aspect of the problem.

The present generation of accelerators, in fact, has already reached an energy at which the phenomena of multiparticle production plays a considerable role. The new generation of accelerators, on the other hand, shifting the center of research in this field from the energy domain of a few GeV to that of several hundred GeV, will make available high quality data on the processes with many particles in the final state which will give us the link with the energy region where cosmic rays data are already known.

From a theoretical point of view, aside from the general need of accounting for the impressive mass of existing data, the interest in these processes

* In this survey, references and notes appear at the end of each chapter.

lies in the realization that multiparticle production processes do not represent a correction to two-body reactions as it would, for instance, be the case in nuclear physics.

In the latter case, actually, many body processes do not appear to contain essentially new infornation on the dynamics of the problem.

In the case of hadronic interactions, on the other hand, the experimental data teach us that, above 10 GeV/c (for the momentum p_{Lab} of the incident particle in the laboratory system), the contribution of many-body events represents, roughly speaking 70% of the total cross section. Furthermore, the most prominent contribution to the elastic scattering (Pomeron exchange) is, very likely, due to the shadow of all the inelastic channels through the mechanism of unitarity.

Also for the latter reason, a better understanding of the dynamics governing the production of many particles is essential in the field of high energy physics. From this point of view, it is very important to make a distinction between the events with n = 2 and n > 2, where n is the number of particles in the final state.

In the present paper, we will mainly concentrate our attention on the processes with $n > 2$ since these, as stated above, are the most relevant ones in the energy region of the new accelerators and of cosmic rays.

The difficulties in proceeding in this direction stem, essentially, from the large number of independent variables that one has to deal with when n particles are present in the final state (3n−4 variables) and in the corresponding problem of organizing the existing data. The latter problem, evidently, originates from the lack of a true theory which could suggest in which direction one should move in this jungle of variables and which set of variables to select as the most signicative one.

The above considerations have been taken into accont in the presentation of the material that follows, and have motivated the choice made in the discussion of the experimental data (Chapter 2). The alternative line of a complete review of the presently available information would have, in our opinion, obscured too much the situation. The same criterion has been followed in the analysis of the kinematical aspects of the problem, i.e., in the study of the phase space and also in the selection of the dynamical models.

2. Review of the Experimental Data in the GeV Region for Hadronic Processes of High Multiplicity

2.1 Total Cross Sections.

The most recent data of the Serpukhov machine[1] seem to indicate that the total cross sections of π^-, K^- and $\bar{p}$ on protons and deuterium remain practically constant in the energy domain corresponding to an incident momentum in the laboratory system (p_{Lab} hereafter) between 20 and 65 GeV/c (see Fig. 1 and Table I). If confirmed, these data put anew the problem of the validity of the Pomeranchuk theorems[2]. A related question is then whether or not the forward scattering amplitude becomes predominantly imaginary at high energy (as well known general arguments based on the unitarity condition would suggest), i.e., if

$$\lim_{E\to\infty} \frac{Re\,F}{ln\,E \cdot Im\,F} \to 0$$

(where F is the scattering amplitude and E the center of mass energy).

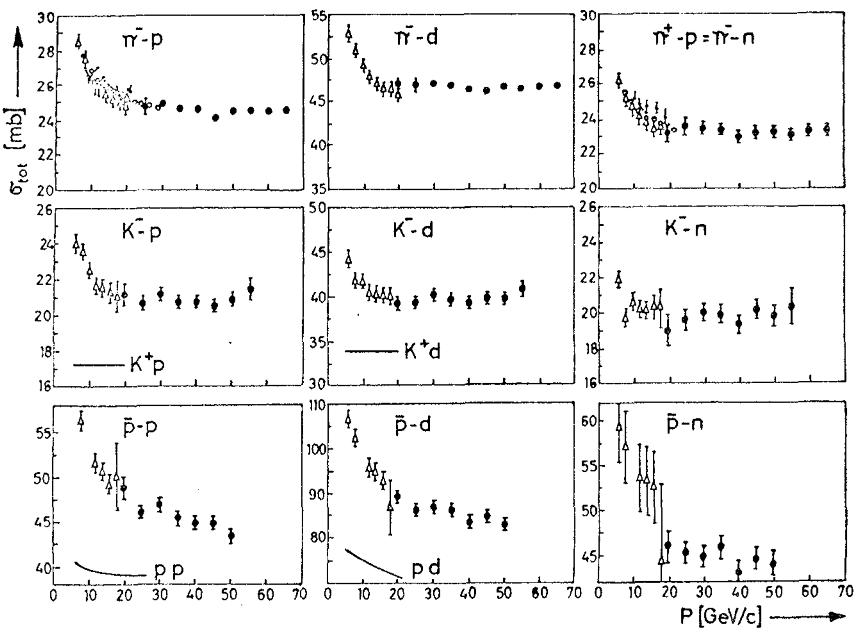

Fig. 1 - Total cross-sections for π^-, K^-, $\bar{p}$ collisions on protons, deuterium and neutrons (From Ref. 1).

Momentum (GeV/c)	Total cross-sections (mb) π^-p	K^-p	$\bar{p}p$	π^-d	K^-d	$\bar{p}d$	π^-n	K^-n	$\bar{p}n$
20	25.38 ± 0.30	21.2 ± 0.6	49.0 ± 1.1	47.28 ± 0.60	39.3 ± 0.6	89.5 ± 1.3	23.3 ± 0.6	19.1 ± 0.8	46.0 ± 1.7
25	24.85 ± 0.25	20.7 ± 0.4	46.1 ± 0.6	47.14 ± 0.50	39.4 ± 0.5	86.5 ± 0.9	23.7 ± 0.5	19.7 ± 0.6	45.3 ± 1.1
30	24.97 ± 0.15	21.3 ± 0.3	47.1 ± 0.6	47.17 ± 0.30	10.4 ± 0.4	87.0 ± 0.9	23.6 ± 0.3	20.1 ± 0.5	44.9 ± 1.1
35	24.75 ± 0.15	20.8 ± 0.3	45.5 ± 0.7	46.85 ± 0.30	39.8 ± 0.4	86.4 ± 1.0	23.5 ± 0.3	19.9 ± 0.5	45.9 ± 1.2
40	24.70 ± 0.15	20.9 ± 0.3	45.0 ± 0.7	46.40 ± 0.30	39.3 ± 0.4	83.5 ± 0.9	23.1 ± 0.3	19.4 ± 0.5	43.2 ± 1.1
45	24.27 ± 0.15	20.6 ± 0.3	44.9 ± 0.7	46.20 ± 0.30	39.9 ± 0.4	84.8 ± 0.9	23.3 ± 0.3	20.2 ± 0.5	44.6 ± 1.1
50	24.62 ± 0.15	21.0 ± 0.4	43.6 ± 0.8	46.63 ± 0.30	39.9 ± 0.5	83.1 ± 0.9	23.4 ± 0.3	19.9 ± 0.6	44.1 ± 1.2
55	24.64 ± 0.15	21.5 ± 0.6		46.44 ± 0.30	40.9 ± 0.8		23.2 ± 0.3	20.4 ± 1.0	
60	24.60 ± 0.15			46.62 ± 0.30			23.4 ± 0.3		
65	24.69 ± 0.20			46.76 ± 0.30			23.4 ± 0.3		

Table I - Results for the measurements of total cross-sections for π^-, K^-, $\bar{p}$ collisions on protons, deuterium and neutrons (From Ref. 1).

2.2 Cross Sections for Inelastic Channels.

It has been observed[3] that the cross section for a given inelastic channel grows, with increasing momentum of the incident particle, from zero (at threshold) to a maximum, and then decreases toward zero as the momentum goes to infinity. In Ref. 3 an attempt has been made to separate the dynamical content of the inelastic cross sections from the dynamical part. This is done by defining the dynamical part of the cross section σ^* as normalized to the Lorentz invariant phase space (L.I.P.S.) for all the inelastic reactions that have been analyzed in $\pi^{\pm}$p, $K^{\pm}$p, pp and $p\bar{p}$ collisions,

$$\sigma^* = \frac{\sigma}{L.I.P.S.} \quad . \tag{2-1}$$

It then follows that, as function of p_{Lab}, σ^* can be described[3] by the simple power law (see Table II)

$$\sigma^* \propto p_{Lab}^{-n} \tag{2-2}$$

where n increases with increasing multiplicity of the final state (see Fig. 2).

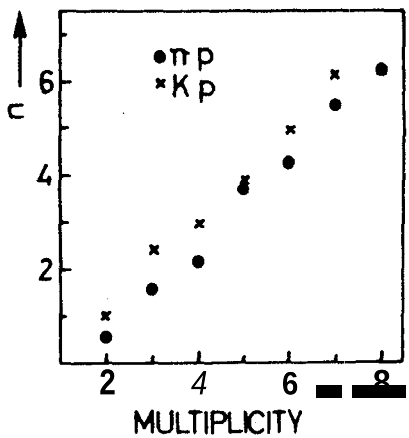

Fig. 2 - Average values of the exponent n in eq. (2.2) for the reactions πp and Kp as functions of the multiplicity (From Ref. 3).

As can be seen from Fig. 2, Eq. (2-2) gives a better interpolation to the data corresponding to channel of high multiplicity as compared to the ones of low multiplicity. This can be attributed to the fact that, in the latter case, resonance production still plays an important role (whereas it becomes inessential in the regime of high multiplicity) and that this resonant effect has not been taken into account in removing the phase space contribution.

Multiplicity	Reaction	Range of p_{lab} in GeV/c	Exponent, n
	$\pi^- p \to p\pi^-\pi^0$	0.7 - 25	1.5 ± 0.05
	$\pi^- p \to n\pi^+\pi^-$	0.6 - 16	1.6 ± 0.1
	$\pi^+ p \to p\pi^+\pi^0$	0.9 - 11.5	1.9 ± 0.05
	$\pi^+ p \to n\pi^+\pi^+$	0.9 - 11.5	1.25 ± 0.1
3	$K^+ p \to pK^0\pi^+$	1.1 - 12.7	2.6 ± 0.05
	$K^+ p \to pK^+\pi^0$	0.9 - 3.5	1.6 ± 0.2
	$K^- p \to p\bar{K}^0\pi^-$	1.1 - 6.0	2.1 ± 0.1
	$pp \to pp\pi^0$	2.8 - 19	1.6 ± 0.15
	$pp \to pn\pi^+$	4 - 28.5	1.6 ± 0.1
	$\pi^- p \to p\pi^+\pi^-\pi^-$	1.9 - 25	2.15 ± 0.05
	$\pi^+ p \to p\pi^+\pi^+\pi^-$	1.1 - 18.5	2.4 ± 0.05
	$K^+ p \to pK^+\pi^+\pi^-$	1.9 - 12.7	3.0 ± 0.05
4	$K^+ p \to pK^0\pi^+\pi^0$	1.9 - 12.7	3.05 ± 0.1
	$K^+ p \to nK^0\pi^+\pi^+$	1.9 - 12.7	3.15 ± 0.15
	$pp \to pp\pi^+\pi^-$	2 - 25	3.05 ± 0.1
	$\bar{p}p \to \bar{p}p\pi^+\pi^-$	2.7 - 7	3.4 ± 0.1
	$\pi^- p \to p\pi^+\pi^-\pi^-\pi^0$	1.9 - 25	3.75 ± 0.05
	$\pi^- p \to n\pi^+\pi^+\pi^-\pi^-$	1.6 - 16	3.65 ± 0.05
	$\pi^+ p \to p\pi^+\pi^+\pi^-\pi^0$	1.8 - 18.5	4.15 ± 0.05
	$\pi^+ p \to n\pi^+\pi^+\pi^+\pi^-$	1.8 - 16	3.0 ± 0.16
5	$K^+ p \to pK^+\pi^+\pi^-\pi^0$	1.6 - 5	3.8 ± 0[illegible]
	$K^+ p \to pK^0\pi^+\pi^+\pi^-$	1.6 - 10	4.3[illegible] ± 0[illegible]
	$K^+ p \to nK^+\pi^+\pi^+\pi^-$	1.9 - 5	3.5 ± 0[illegible]
	$K^- p \to pK^-\pi^+\pi^-\pi^0$	3 - 12.7	3.7 ± 0[illegible]
	$pp \to pp\pi^+\pi^-\pi^0$	2.2 - 10	4.2 ± 0.1
	$pp \to pn\pi^+\pi^+\pi^-$	2.2 - 10	4.6 ± 0.15
	$\pi^- p \to p\pi^+\pi^+\pi^-\pi^-\pi^-$	2.7 - 16	4.25 ± 0.1
	$\pi^+ p \to p\pi^+\pi^+\pi^+\pi^-\pi^-$	2.7 - 8.5	4.3 ± 0.25
6	$K^+ p \to pK^+\pi^+\pi^+\pi^-\pi^-$	3 - 8.3	5.25 ± 0.2
	$K^+ p \to pK^0\pi^+\pi^+\pi^-\pi^0$	2.7 - 8.3	4.75 ± 0.15
	$pp \to pp\pi^+\pi^+\pi^-\pi^-$	5.6 - 28.5	5.6 ± 0.2
	$\bar{p}p \to \bar{p}p\pi^+\pi^+\pi^-\pi^-$	5.7 - 7	4.1 ± 1.4
	$\pi^- p \to p\pi^+\pi^+\pi^-\pi^-\pi^-\pi^0$	5.5 - 16	5.6 ± 0.2
	$\pi^- p \to n\pi^+\pi^+\pi^+\pi^-\pi^-\pi^-$	5.5 - 16	5.8 ± 0.2
	$\pi^+ p \to p\pi^+\pi^+\pi^+\pi^-\pi^-\pi^0$	3.4 - 8.5	5.8 ± 0.3
7	$\pi^+ p \to n\pi^+\pi^+\pi^+\pi^+\pi^-\pi^-$	3.5 - 8	4.5 ± 0.3
	$K^+ p \to pK^+\pi^+\pi^+\pi^-\pi^-\pi^0$	3.5 - 8.3	6.2 ± 0.4
	$pp \to pp\pi^+\pi^+\pi^-\pi^-\pi^0$	5.5 - 28.5	5.95 ± 0.1
	$pp \to pn\pi^+\pi^+\pi^+\pi^-\pi^-$	5.5 - 28.5	6.25 ± 0.2
8	$\pi^- p \to p\pi^+\pi^+\pi^+\pi^-\pi^-\pi^-\pi^-$	10 - 16	6.3 ± 0.9

Table II - Power law fit, Eq. (2-2), for inelastic reactions $\pi^\pm p$, K^+p, pp, $p\bar{p}$; values of the exponent (From Ref. 3).

2.3 Topological Cross Sections (Charged Prongs)

An interesting way of describing production processes is through the use of topological cross sections. In the case, the inelastic events are classified in terms of the total number of charged particles in the final state of a given reaction and the term topological cross section refers to the sum of all those reactions which contribute to a given topology[4].

Some of the best data in what concerns topological cross sections are the Brookhaven data[5] for pp collision where the events are analyzed with four or more charged particles in the final state in the interval of p_{Lab} between 13 and 28.5 GeV/c (more precisely, at 12.88, 18.00, 21.08, 24.12 and 28.49 GeV/c). The events are combinations of the various reactions

$$pp \to pp + m(\pi^+\pi^-) + \text{neutral pions},$$

$$pp \to pn + \pi^+ + m(\pi^+\pi^-) + \text{neutral pions},$$

$$pp \to nn + 2\pi^+ + m(\pi^+\pi^-) + \text{neutral pions},$$

with $m \geqslant 1$.

The results of these analyses for the topological cross sections (versus p,,,,) are given in Fig. 3 (see Fig. 4 for a comparison with the data of other experiments[6]).

Some general conclusions can be drawn from the above data

a) the topological cross sections for 4, 6, 8 charged prongs level at constant values with increasing p_{Lab} (of course, it is an entirely open question whether or not they will eventually tend to zero as $p_{Lab} \to \infty$);

b) at *28.5* GeV/c the following relation holds

$$\sigma_4 \simeq 2\sigma_6 \simeq 4\sigma_8 \, ; \tag{2-3}$$

c) the topological cross sections for higher multiplicity increase with p_{Lab} (this is to be expected since in this case there is less energy available for each particle than in the case of lower multiplicity).

On the basis of these observations, Wroblenski[7] has proposed a phenomenological formula giving a universal energy dependence of all the topo-

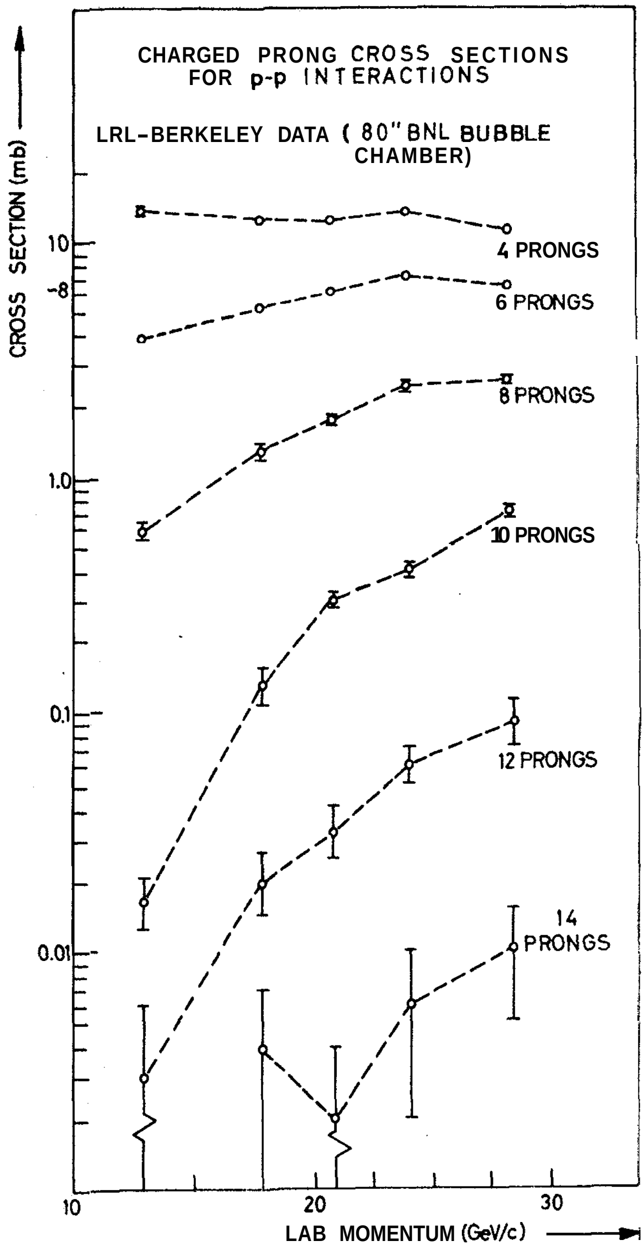

Fig. 3 - Charged prong cross-sections for *pp* interactions at 12.88 GeV/c, 18.00 GeV/c, 21.08 GeV/c, 24.12 GeV/c, 28.49 GeV/c bearn mornenta (Frorn Ref. 5 and 27).

logical cross sections considered. In fact, plotting these cross sections as functions of the *c.m.* energy for pair of charged particles, one finds

$$\sigma_{2(k+1)} = \tfrac{1}{2}\,\sigma_{2k} \tag{2-4}$$

(when the measurement is made at the same *c.m.* energy for pair).

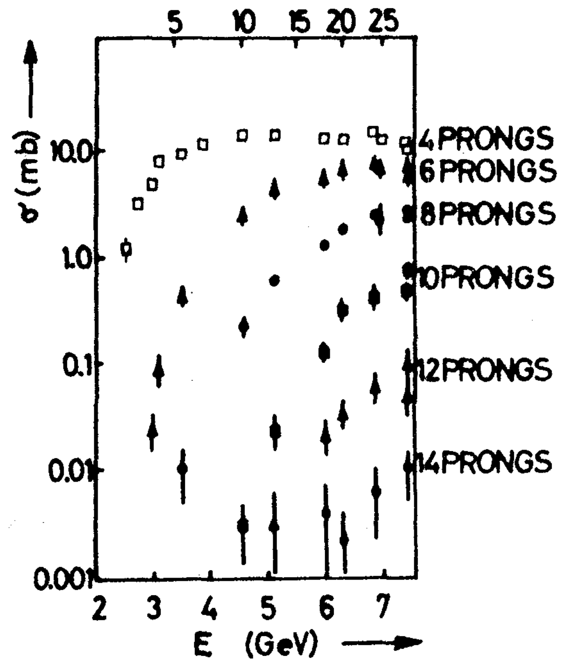

Fig. 4 - *pp* topological cross-sections as a function of the beam momentum and c.m. energy (From Ref. 7).

Thus, at the present energies the data are suggestive of the "2^{-k} law", namely, the production cross sections for creation of one, two, three,... pairs of charged particles are in the ratio $1 : 2^{-1} : 2^{-2} : \ldots$ when measured at the same *c.m.* energy for pair of particles.

This gives the empirical rule ($k > 3$)

$$\sigma_{2(k+1)} \times \sigma_{2(k-1)} = \sigma_{2k}^2 \tag{2-5}$$

(see Fig. 5 and Fig. 6).

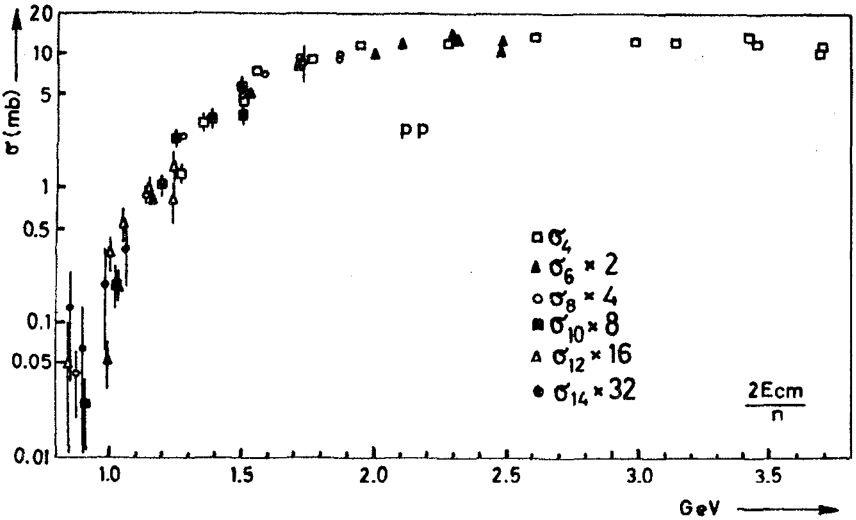

Fig. 5 - *pp* topological cross-sections as a function of the beam momentum and c.m. energy per pair of charged particles, $2E_{c\,m}/n$, n = prong number (From Ref. 7).

On the other hand, from the data in Figs. 3 and 4, one sees that σ_4 tends to a maximum and then decreases very smoothly. From the 2^{-k} law, one tentatively concludes that all the topological cross sections tend to a limiting value. In fact, from the *assumption* that the 2^{-k} law is valid, one would have that all the topological cross sections σ_4, σ_6, σ_8 etc. must go to constant values. Should this not be the case, the total inelastic cross section would simply be given by σ_2 since all the other cross sections would tend to zero with energy. If a limiting value is attained, one has, on the other hand,

$$\sigma_{in} = \sigma_2 + \sigma_4 + \sigma_6 + \ldots = \sigma_2 + \sigma_4 \sum_{k=0}^{\infty} 2^{-k} = \sigma_2 + 2\sigma_4 . \qquad (2\text{-}6)$$

These observations, however, deserve further investigation. In particular, the 2^{-k} law predicts a limiting constant value for the average multiplicity which does not seem to be in agreement with the experimental data (see Sec. 2-4).

Thus, whereas the 2^{-k} law seems to be empirically well established at the present energies, doubts can be raised relatively to its attendibility at all energies.

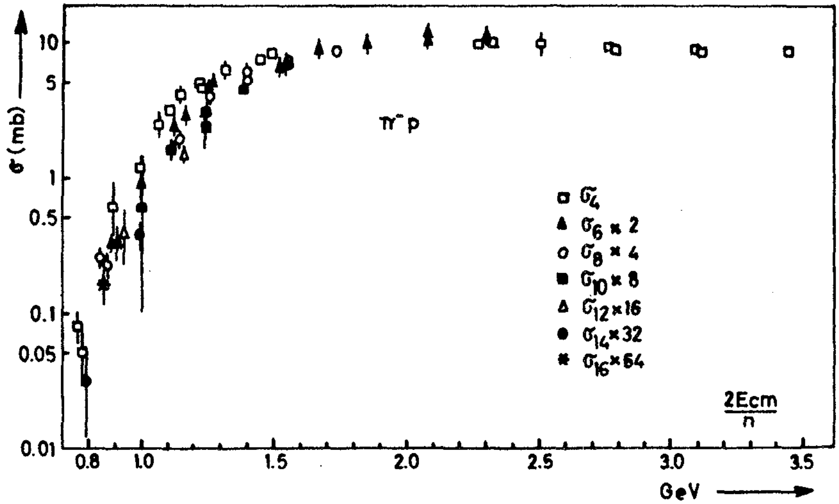

Fig. *6* - $\pi^- p$ topological cross-sections as a function of the c.m. energy per pair of charged particles (From Ref. 7).

No. Of Charged Prongs	σ (mb)	
	Total	Partial
2	6.5	$pn\pi^+$ (1.5 ± .1) $\Delta^{++}n$ (0.115 ± 0.015)
4	10.5	$pp\pi^+\pi^-$ (1.1 ± .1) $\Delta^{++}p\pi^-$ (0.8 ± .1)
6	5.5	$ppn^+\pi^-\pi^+\pi^-$ (0.38) $\Delta^{++}\pi^-\pi^+\pi^-p$ (~ 0.2)
8	2.4	$pp\pi^+\pi^-\pi^+\pi^-\pi^+\pi^-$ (0.115)
10	0.45	$pp\pi^+\pi^-\pi^+\pi^-\pi^+\pi^-\pi^+\pi^-$ (0.02)
12	0.05	$pp\pi^+\pi^-\pi^+\pi^-\pi^+\pi^-\pi^+\pi^-\pi^+\pi^-$ (0.002)

Table III - Cross-sections for *pp* at 28.5 GeV/c. (Frorn Ref. 27).

The results previously quoted (Refs. 5 and 7) agree with those of Ellis *et al.*[8] and of Connolly et *al.*[9] at 28.5 GeV/c for the lab. momentum of the incident proton (see Table III where, together with the values of the topological cross sections for 2, 4, ... charged prongs, are given the individual cross sections for production of pairs of $\pi^+ \pi^-$ without $\pi_0's$ in the single channels).

Some conclusions which follow from Table III are in order: a) for p_{Lab} between 10 and 30 GeV/c, 3/4 of the proton-proton total cross section are due to the channels with 2, 4 and 6 prongs; b) the individual cross sections (without $\pi_0's$ in the final states) become negligible, with increasing multiplicity, as compared to the total cross section.

2.4 Average Multiplicity as Function of Energy.

The average multiplicity is defined as

$$\langle n \rangle = \frac{\sum_{n=1}^{\infty} n\sigma_n}{\sum_{n=1}^{\infty} \sigma_n} \tag{2.7}$$

where now σ_n denotes the cross section for production of n particles in the final state (and not the topological cross sections discussed previously). Certainly, (n) is function of energy and the experimental data (see below) suggest that it is a growing function of energy.

The information on the energy dependence of (n) comes either from theoretical models or from the interpolation of the data connecting the cosmic-ray energy range with that of the accelerators.

The various theoretical models suggest:

A) Statistical models[10]: $\langle n \rangle \propto s^{1/4}$ (2-8)

B) Multiperipheral models[11,12]: $\langle n \rangle \propto \ln s$ (2-9)

C) Isobar models[13]: $\langle n \rangle \propto s^{1/2}$ (2-10)

D) Wroblenski mode1[7]: $\langle n \rangle \propto \text{const.} \simeq 6$ (2-11)

where s is the squared *c.m.* energy.

In the energy interval covered by the present accelerators, it is very difficult to distinguish between the various behaviors (2-8,11) even though the indications seem to point toward the suggestions of models of type A) or B). The data from the new generation of accelerators, however, will be necessary to clarify the situation.

Concerning the interpolation between accelerator and cosmic ray data, one should be aware of the ambiguities inherent in the procedure of interpolating between data of so different origin. We will, however, quote a few interpolating formulae that have been proposed by different groups.

Mc Cusker and Peak[14] suggest (in the range $16 \lesssim E \lesssim 2800$ GeV)

$$(n,) \simeq 4.1\, ln\, [E/ln\, 16] \qquad (2\text{-}12)$$

(where n_s is the number of secondaries and all units are in GeV).

Yamada and Koshiba[15] suggest either

$$(n,) \simeq 4.4\, ln\, [E/3] \qquad (2\text{-}13)$$

or

$$\langle n_s \rangle \simeq 2.8\, E^{1/4}. \qquad (2\text{-}14)$$

These interpolations are to be compared with the more recent result of Jones *et al.*[16] (Echo Lake experiment) which give for the average multiplicity of charged particles

$$(n,) \simeq (1.41 \pm .20)\, ln\, Q + (2.04 \pm .19), \qquad (2\text{-}15)$$

where Q is the *c.m.* energy available for each particle produced and the data refer to *pp* collisions in the energy range between *90* and *800* GeV.

From the above considerations, it seems that rhe average multiplicity increases and that the logarithmic growth *(2-9)* is preferred.

It is worthwhile to mention that the 2^{-k} law discussed in Sec. (2.3), if assumed valid at all energies, leads to a constant multiplicity of charged particles since[17]

$$\langle n_c \rangle \simeq \frac{\sum_{k=2}^{\infty} 2k\sigma_{2k}}{\sum_{k=2}^{\infty} \sigma_{2k}} \simeq \sum_{k=2}^{\infty} k2^{2-k} = 6. \qquad (2\text{-}16)$$

The previous considerations show that the average multiplicity is a parameter which can be crucial in discriminating between the various theoretical models, i.e., between the various dynamical assumptions which, through specific mechanisms for the description of strong interactions at high energy, lead to the different predictions for $\langle n \rangle$ of the kinds previosly mentioned (Eqs. (2-8,11))[18].

As a final observation, we notice that the fluctuations around the average number of particles emitted at a given energy are expected to be fairly large (for example, in the RNL experiment at 28.5 GeV/c an event with 16 prongs has been seen among $\sim$ 1500 collisions). This seems to be confirmed by the cosmic ray data. For instance, between .5 and 2 TeV, the average multiplicity is[15]

$$\langle n_s \rangle \simeq 11.2 \pm 2.1. \tag{2-17}$$

In the same range, the variance (or dispersion)

$$D^2 = \langle n^2 \rangle - \langle n \rangle^2 \tag{2-18}$$

$$D \simeq 9.7. \tag{2.19}$$

2.5 Multiplicity Distribution

Another important parameter in order to discriminate between the various models is the multiplicity distribution which gives the number of times that a given number of secondaries is produced in a high energy collision.

Brandt[19] has interpolated the data for $\pi^- p$ (see Fig. 7) with a Poisson distribution

$$P_n(\langle n \rangle) = \frac{\langle n \rangle^n}{n\,!}\, e^{-\langle n \rangle} \tag{2-20}$$

(where $\langle n \rangle$ is the total average multiplicity) and he finds that this interpolation compares favorably with the data at 4, 8, 10 and 16 GeV/c.

The same kind of distribution obtains in statistical-like models[10] and is assumed in multiperipheral Regge models".

Along this line, C.P. Wang has proposed a model[20] with a distribution essentially analogous to that of Ref. 19 but where the multiplicity refers

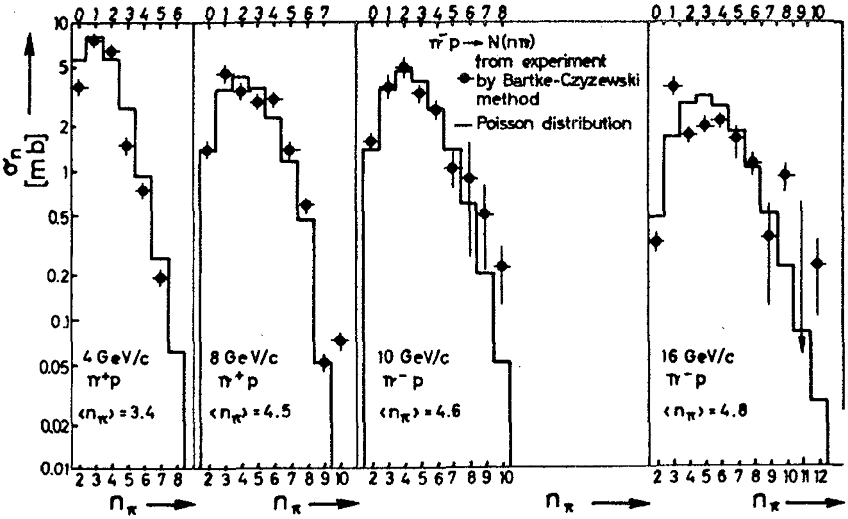

Fig. 7 - Distributions of the number of secondary pions produced in $\pi^{\pm}p$ interactions compared to Poisson distributions (From Ref. 19).

to the pairs of charged particles only and he obtains satisfactory agreement with the data. However, it has been pointed out by Czyzewski and Rybicki[21] that the experimental data used in Ref. 20 are of low quality so that the conclusions drawn should be taken with caution. Moreover, in Ref. 21 it is concluded that a Poisson distribution is not consistent with good quality data. This is shown by introducing a parameter which is the ratio of the mean multiplicity and the dispersion of the distribution of charged prongs. More precisely, one defines

$$x = \frac{n_{\pm} - \langle n_{\pm} \rangle}{D} \tag{2-21}$$

and

$$y = DP(n_{\pm}), \tag{2-22}$$

where D has been defined in Eq. (2-18) and $P(n_{\pm})$ is the experimental fraction of events with charged prongs.

Fig. 8 shows the deviation of the experimental data from the predictions of the Poisson distribution. The disagreement is not surprising, however, if one remembers the remark made at the end of Sec. (2.4) and if one recalls

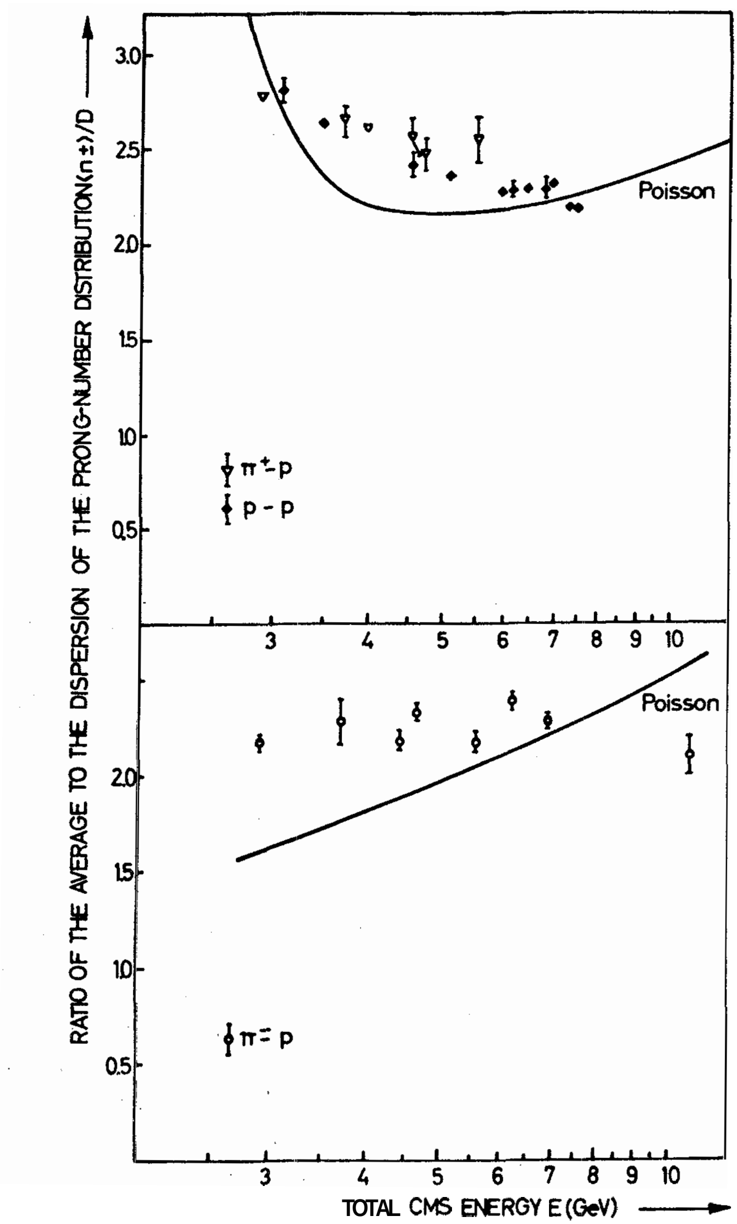

Fig. 8 - The ratio of the average multiplicity (n,) to the dispersion (see eq. 2.18) of the prong number distribution as a function of c.m. energy. The curves represent $\langle n_{\pm}\rangle/D$ calcuiated from the Poisson distribution (From Ref. 21).

that the dispersion predicted by a Poisson distribution is $\langle n,\rangle$. It is clear then that a large fluctuation like the one of Eq. (2.19) cannot be given by a Poisson distribution.

Czyzewski and Rybicki observed also that the formula

$$y = 2de^{-d^2} \frac{d^{2(dx+d^2)}}{\Gamma(dx + d^2 + 1)} \tag{2-23}$$

interpolates very well all the data in the distributions for the various production processes in $\pi^{\pm} p$ and pp collisions at different energies (see Fig. 9). In Eq. (2.23), d is a free parameter ($\simeq$ 1.8) and the formula itself is the generalization of what one would obtain from Eq. (2.20) when one replaces the factorial with a gamma function for non integer values of its argument.

More recently, Horn and Silver[22] tackled the problem of calculating the statistical distribution of pions in a production process where the charge is conserved[23]. They find

$$P_n(z) = [J_0(2iz)]^{-1} \frac{z^{2n}}{(n!)^2} \tag{2-24}$$

where J_0 is the Bessel function of zero order. The corresponding expression for the mean multiplicity $\langle n\rangle$ is

$$\langle n \rangle = -izJ_1(2iz)/J_0(2iz) \tag{2-25}$$

which gives the relation between $\langle n\rangle$ and z. The agreement with the data is good but the data used are the same as in Ref. 20 so that the same criticism applies.

It is interesting to notice that the use of a Poisson distribution has' been criticized also from a theoretical point of view[24]. Speciiically, one can show that models that predict Poisson distributed scattering processes are inconsistent with the requirement that total cross sections should asymptotically become constant (or grow with energy) and violate general bounds if the multiplicity increases faster than a dilogarithmic function of energy.

To see how this comes about, notice that, from Eq. (2.20) one has

$$\sigma_{el} = \sigma_{tot} e^{-\langle n \rangle}. \tag{2-26}$$

On the other hand, a bound by **Martin**[25] requires that

$$\sigma_{el} \gtrsim C \frac{\sigma^2_{tot}}{ln^2(s/s_0)} \qquad (2\text{-}27)$$

where C is a (positive) constant and s_0 a scale parameter.

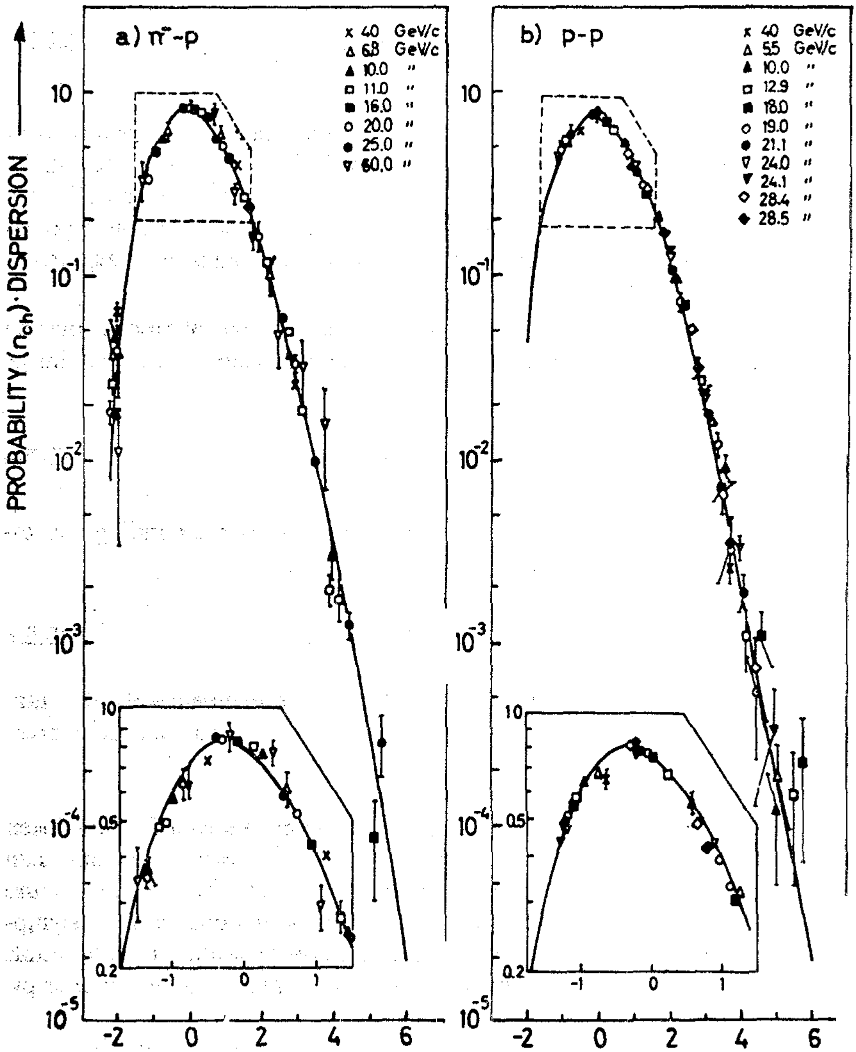

Fig. 9 - Experimental prong number distributions fitted by formula (2.23) (From Ref. 21).

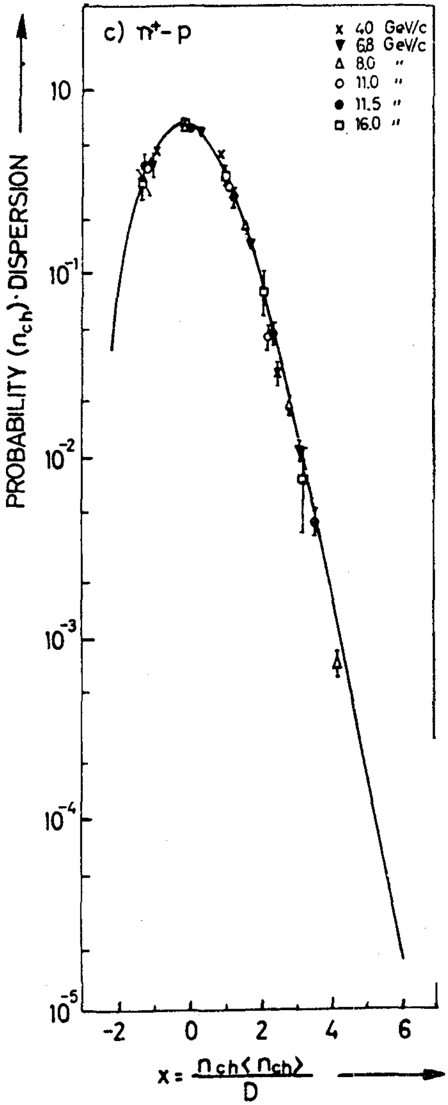

Fig. *9* (cont.)

Combining Eqs. (2.26, 27) one gets

$$\ln a_n \leqslant 2 \ln \ln (s/s_o) - \langle n \rangle - \ln C. \tag{2-28}$$

Thus if a_n does not decrease with energy as $s \to \infty$, we must have

$$\langle n \rangle \leqslant 2 \ln \ln (s/s_o) \tag{2-29}$$

which, as previously discussed, is in contradiction with the experimental information on the rate of growth of $\langle n \rangle$.

2.6 Longitudinal and Transverse Momentum Distributions of Secondaries

It has been shown[26] that the angular distribution with respect to the momentum of one of the outgoing particles is factorizable as function of the longitudinal (p_L) and transverse (p_T) components of the *c.m.* momentum. This implies that

$$d^2\sigma/d\Omega dp = F(p_L)\,G(p_T) \tag{2-30}$$

(see Fig. 10a) where p, p_L and p_T refer to any of the outgoing particles.

This observation follows from the consideration that the behavior of the curves given in Fig. 10a, for three different values of p_T as function of p_L, is essentially the same,

In the same experiment[26], measurements have been made for very small values of p_T. A very narrow forward peak has thus been found for production of π^+'s as well as of π^-'s. This peak can be simulated by

$$\frac{d^2\sigma}{d\Omega\,dp} \propto \exp[-15p_T^2]. \tag{2-31}$$

Fig. 10b shows the behavior of the angular distribution in p_T at fixed p_L.

Another set of data relative to the angular distributions as functions of p_L and p_T is given for pp collision[6,27] at 28.5 GeV/c (see Figs. 11,12) and for K_p^+[27] at 12.7 GeV/c (see Fig. 13).

From Figs. 10-13 and Table IV, useful information can be derived on the behavior with respect to p_L and p_T in the various channels[27]:

a) Properties with Respect to $\mathbf{p}_L$

i) In the reactions

$$p + p \to p + anything, \tag{2-32}$$

$$K^+ + p \to K^+ + anything, \tag{2-33}$$

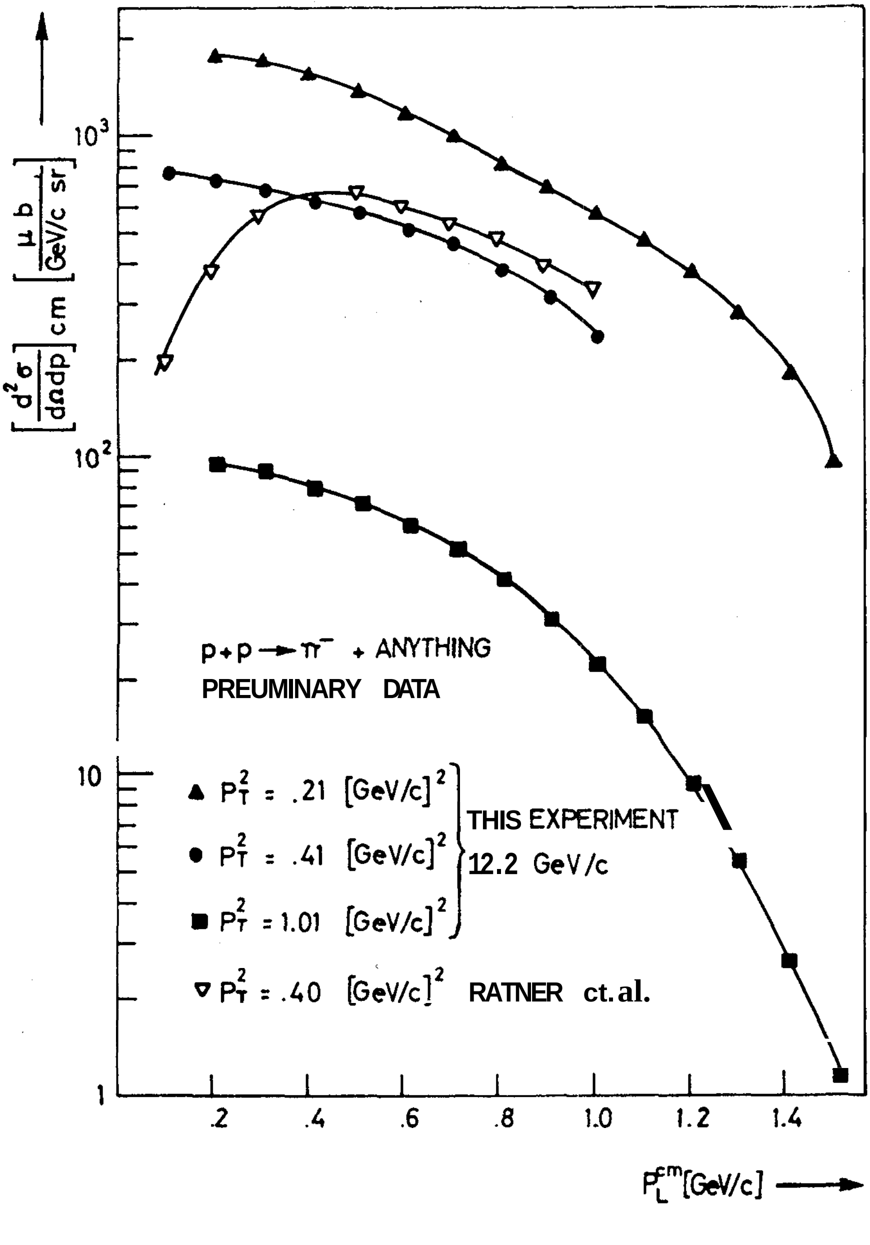

Fig. 10a - Angular distributions at fixed p_T as function of $p_L^{c.m.}$ for $\pi^\pm$ from the reaction $pp \to \pi^\pm + anything$ (From Ref. 26). See next page (cont. Fig. 10a).

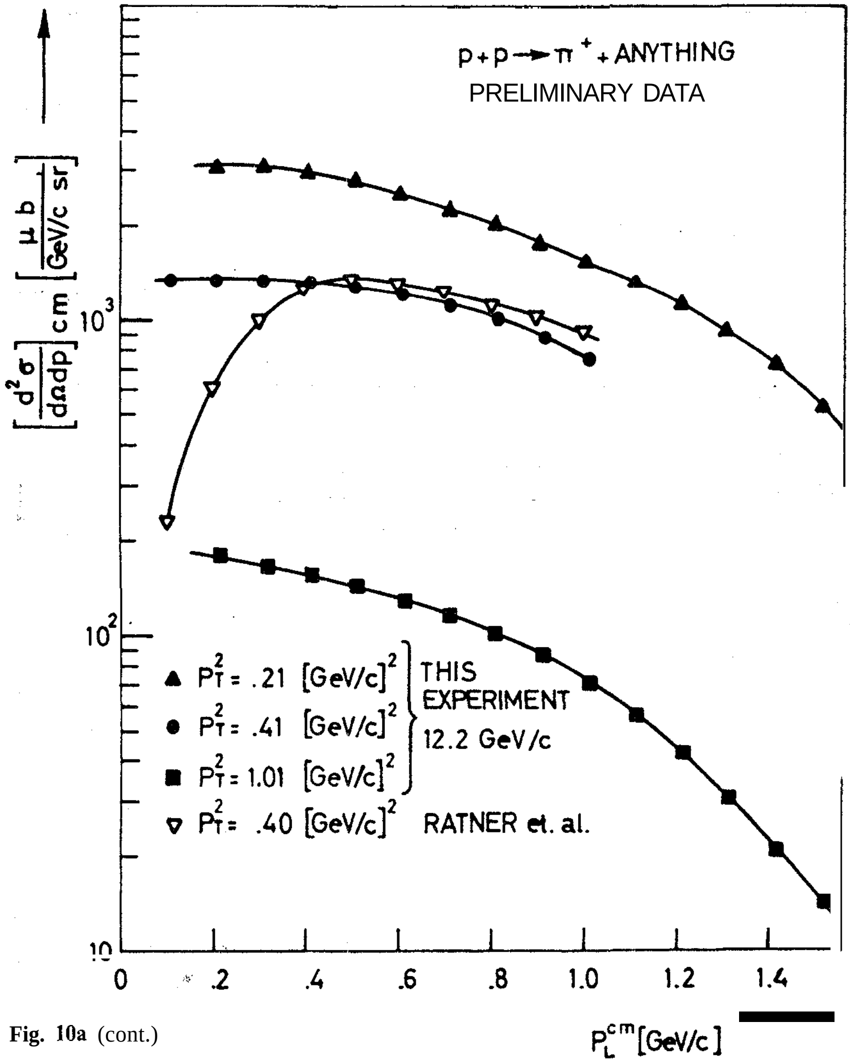

Fig. 10a (cont.)

the mean value $\langle p_L \rangle$ of the outgoing proton and kaon respectively are larger than for the produced pions.

ii) In the case of reaction (2.32), the mean value $\langle p_L \rangle$ of the outgoing proton decreases with increasing multiplicity.

iii) For reaction (2.32) the p_L distribution of the pions produced has a maximum at $p_L = 0$.

iv) The mean value (p,) of the outgoing pions decreases with increasing multiplicity.

b) Properties with Respect to p_T

i) The distributions in p_T have behaviors very similar for the various'

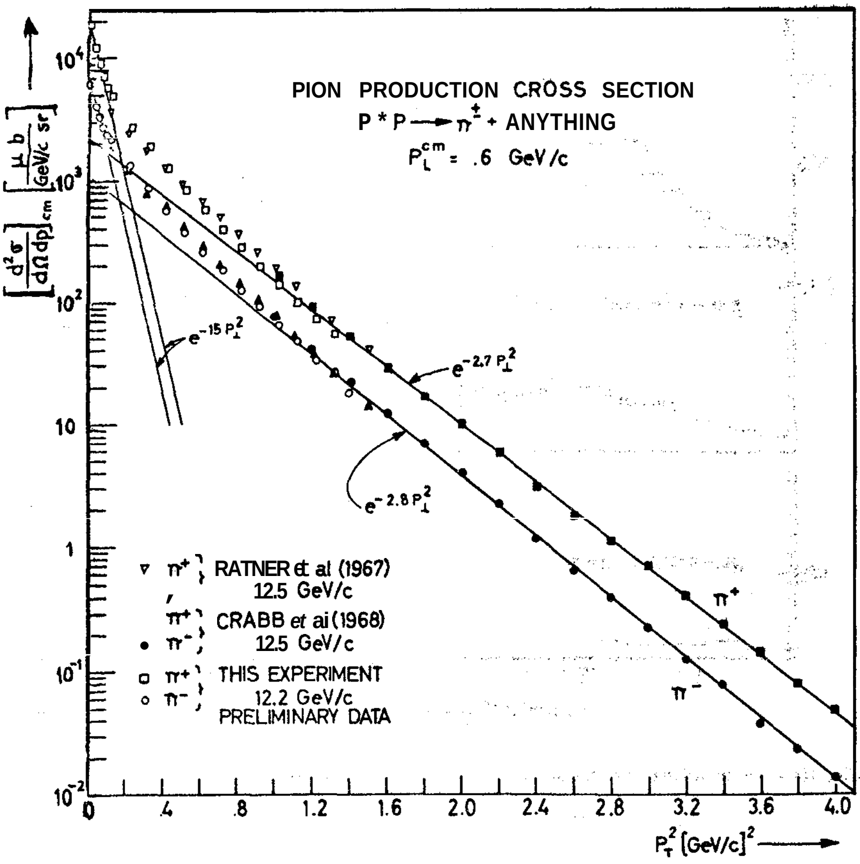

Fig. 10b - Angular distributions at fixed p_L^{cm} as function of p_T from the reaction pp → $\pi^\pm$ + *anything* (From Ref. 26).

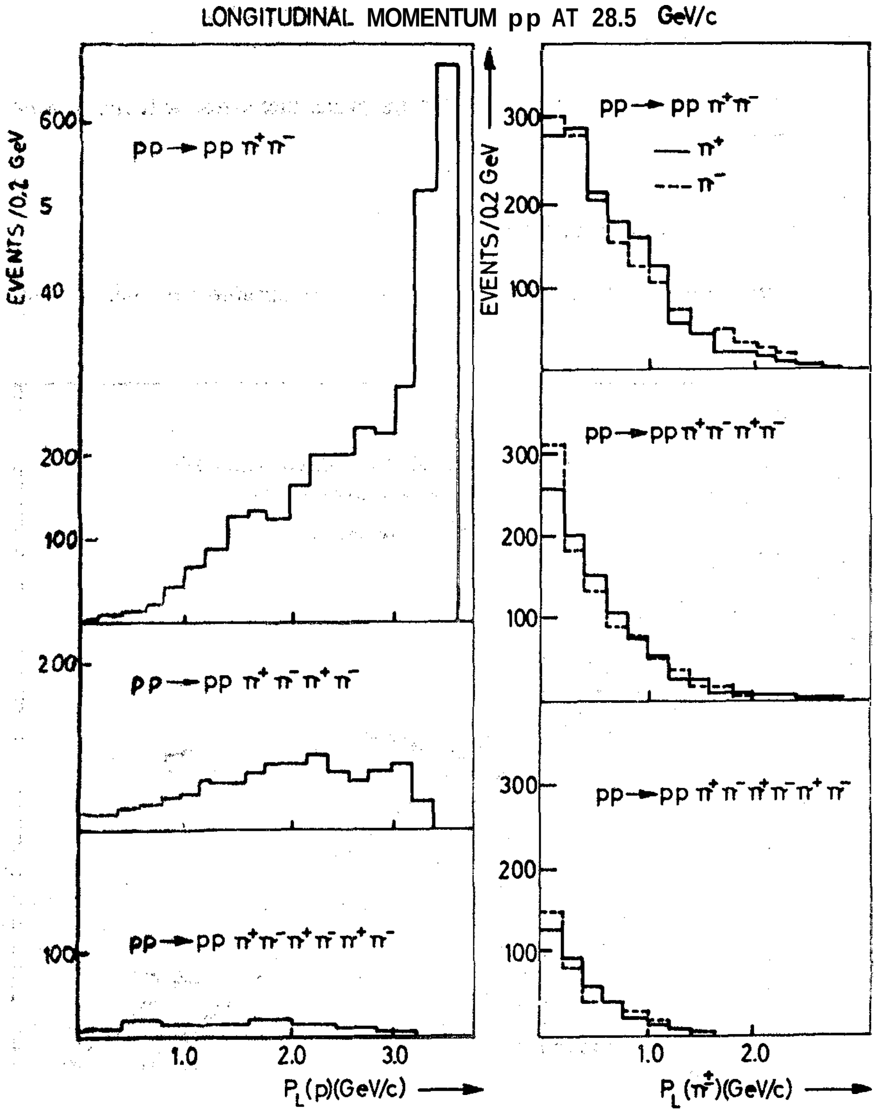

Fig. 11 - Center-of-mass longitudinal distributions for protons and $\pi^\pm$ from the reactions

$$pp \rightarrow pp\,\pi^+\pi^-$$
$$pp \rightarrow pp\,\pi^+\pi^-\pi^+\pi^-$$
$$pp \rightarrow pp\pi^+\pi^-\pi^+\pi^-\pi^+\pi^-,$$

at 28.5 GeV/c (From Ref. 27)

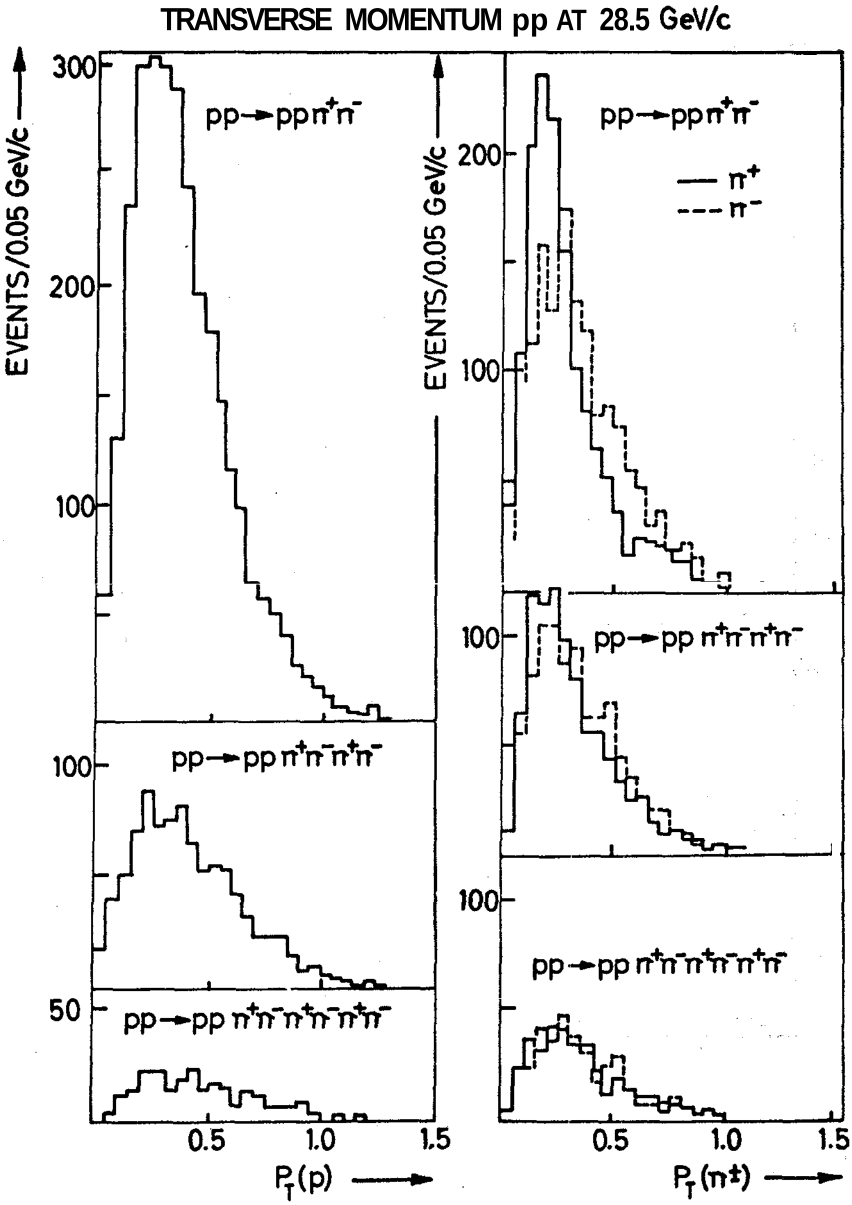

Fig. 12 - Center-of-mas~transverse momentum distributions for protons and $\pi^{\pm}$ from reactions $pp \to pp\,\pi^+\pi^-$ $pp \to pp\,\pi^+\pi^-\pi^+\pi^-$ $pp \to pp\,\pi^+\pi^-\pi^+\pi^-\pi^+\pi^-$

at 28.5 GeV/c. (From Ref. 27).

kinds of outgoing particles (contrary to what happens for the V, distributions).

ii) $\langle p_T \rangle$ increases very slowly with increasing multiplicity (actually, it stays nearly constant for the pions whereas a slight increase is noticed for the proton).

iii) The mean value $\langle p_T \rangle$ is relatively independent of the energy of the incident particle.

These observations relative to $\langle p_T \rangle$ support the observation that in the *c.m.* system the particles produced are distributed in two narrow cones along the forward and backward directions. In the laboratory system, this corresponds to having two cones, a narrow one along the direction of flight of the incident particle (the forward cone of the *c.m.*) and a diffuse one (the backward cone of the *c.m.*).

The different behaviors of rhe outgoing proton (or kaon) as compared to the other particles produced (mostly pions), lead to the suggestion that the former should be considered as "leading particles". This is consistent with the observed smallness of the inelasticity (i.e., the fraction of energy which the incident particle looses in the production process). For instance, at $E_{c.m.} \simeq 30$ GeV (where $E_{c.m.}$ is the total center of mass energy), we have for the mean value of the *c.m.* energy of a produced pion[28]

$$\langle E_\pi \rangle \simeq .08\, E_{c.m.} \,. \tag{2.34}$$

The above ratio is a slowly varying function of $E_{c.m.}$ (consistent with $E_{c.m.}^{1/2}$). On the other hand, for the outgoing proton, we have

$$\langle E_p \rangle \simeq .3\, E_{c.m.} \,. \tag{2-35}$$

Other information can be obtained[5] from the analysis of the p_T and p_L distributions of an outgoing pion for a given charge configuration in the final state at a given incident momentum. These distributions, normalized to the total number of tracks N_{tot}, are interpolated by

$$dN/dp_T = (4/3) N_{tot}\, \pi^{-1/2} a_T^{5/2} p_T^{3/2} \exp(-a_T p_T) \tag{2-36}$$

and

$$dN/dp_L = N_{tot}\, a_L \exp(-a_L p_L). \tag{2-37}$$

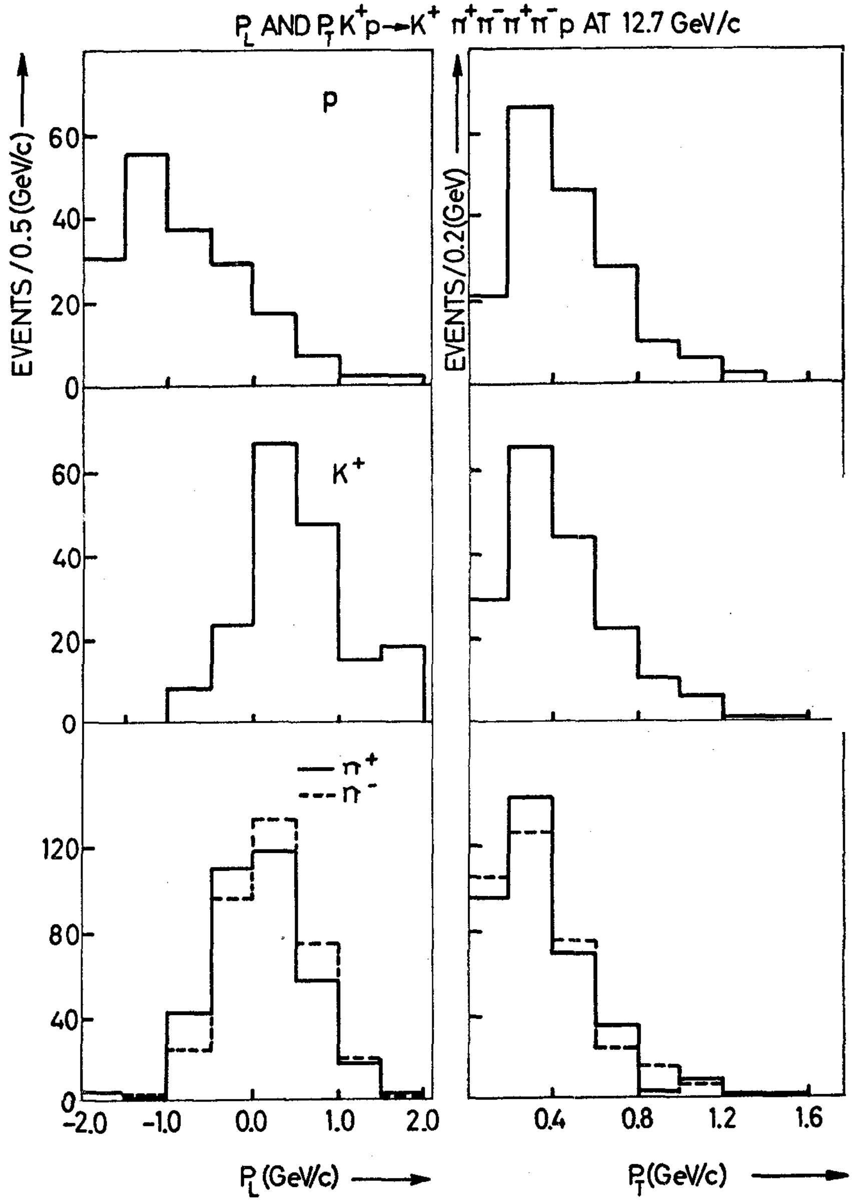

Fig. 13 - Center-of-mass longitudinal, p_L, and transverse, p„ distributions for proton, K^+, $\pi^\pm$ in the reaction $K^+p \rightarrow K^+\pi^+\pi^-\pi^+\pi^-p$, at 12.7 GeV/c (From Ref. 27).

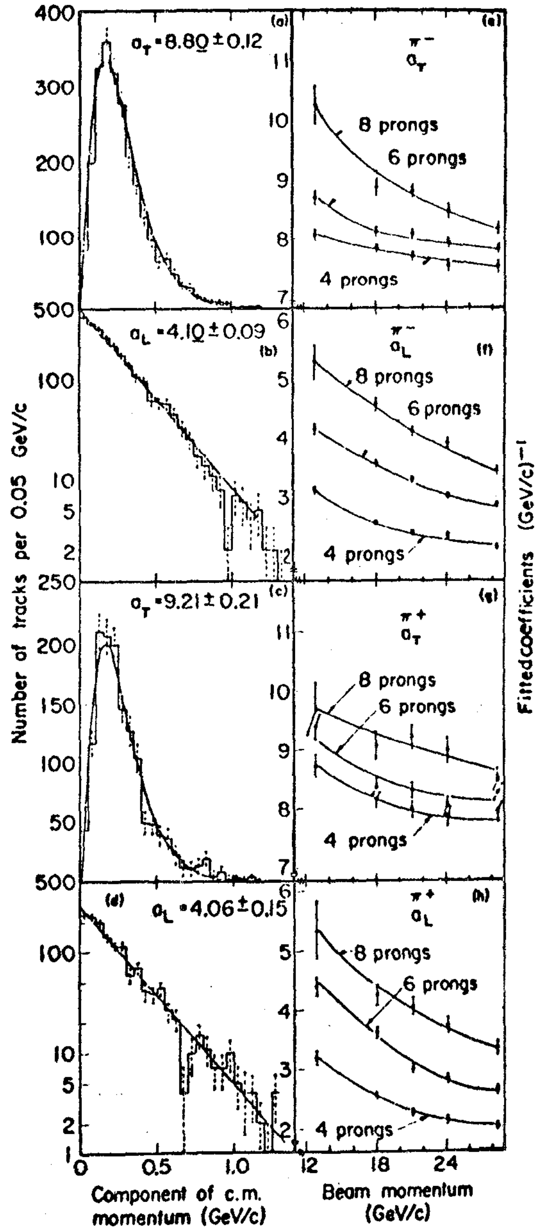

Fig. 14 - Fits to the p_L and p_T distributions for π^- and π^+ produced in pp collisions (a, b, c, d). Dependence of fitted parameter on beam momentum and multiplicities (e. f, g. h). (From Ref. 5).

The distribution in p_L is suggested by a description of the production process in terms of a thermodynamical model. The parameters a, and a, in Eqs. (2.36, 37) vary with the multiplicity and with the energy. The situation is illustrated in Fig. 14.

pp At 28.5 GeV/c

	$<p_L>$			$<p_T>$			
	p	π^+	π^-	p	π^+	π^-	EVENTS
$pp \to pp\pi^+\pi^-$	2.71 ± .05	.64 ± .02	.68 ± .02	.37 ±.02	.28 ±.01	.36 ±.01	1450
$\to pp\pi^+\pi^-\pi^+\pi^-$	1.99 ±.07	.55 ±.02	.52 ±.02	.40 ±.02	.32 ±.01	.35 ±.01	470
$\to pp\pi^+\pi^-\pi^+\pi^-\pi^+\pi^-$	1.41 ±.11	.41 ±.03	.40 ±.03	.48 ±.04	.35 ±.02	.34 ±.02	125

K^+p At 12.7 GeV/c (179 Events)

	$<p_L>$				$<p_T>$			
	p	K^+	π^+	π^-	p	K^+	π^+	π^-
$K^+p \to K^+p\pi^+\pi^-\pi^+\pi^-$	-1.0	.61	.44	.40	.46	.44	.36	.36

Table IV - Average values of p_L and p_T in pp at 28.5 GeV/c and in K^+p at 12.7 GeV/c (From Ref. 27).

2.7 Pionization.

Another important experimental aspect of hadronic interactions of high multiplicity which we finally wish to discuss briefly, concerns the relative abundance of the different kinds of particle produced. As already mentioned previously, it is well known that the production of pions represents the most relevant part of these processes.

Fig. 15a gives the variation of N_{K^-}/N_{π^-} and of $N_{\bar{p}}/N_{\pi^-}$ as function of the incident beam momentum. The data refer to small angle proton-aluminum collisions with an incident energy of about 70 GeV (Serpukhov-Cern collaboration). Fig. 15b gives the same quantities as function of the incident beam momentum divided by the maximum momentum p_{max} kinematically allowed to the heaviest particle (K^- and $\bar{p}$) at various energies.

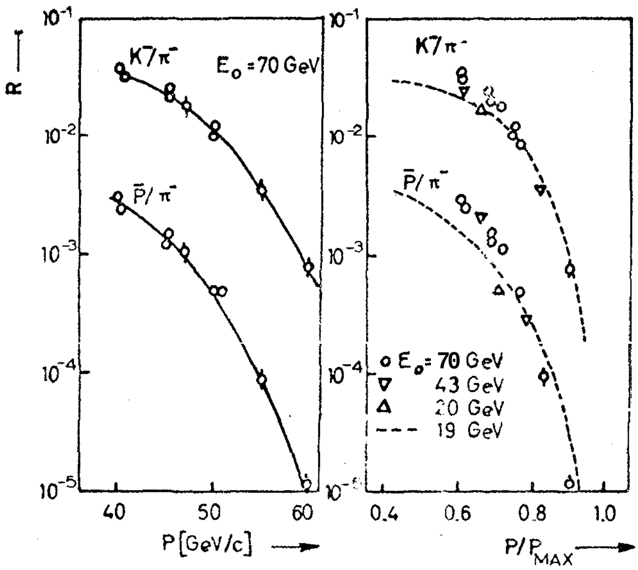

Fig. 15a - Particle ratios R, measured at 70 GeV incident energy, versus beam laboratory-momentum. (From Ref. 29).

Fig. 15b - Particle ratios versus beam laboratory-momentum divided by the kinematically allowed maximum momentum of the heavier particle, K^- and $\bar{p}$ respectively. (From Ref. 29).

Some general conclusions on the ratios N_{K^-}/N_{π^-} and $N_{\bar{p}}/N_{\pi^-}$ between the number of particles of different kinds produced can be drawn[29] (see Figs. 15a,b and Table V):

i) they decrease considerably with increasing momenta (two orders of magnitude in an interval of 20 GeV/c);

ii) in the angular interval considered, they are independent of the angle;

iii) plotted vs. the variable p/p_{max}, they look similar[31] in the limit $p \to p_{max}$ for collisions at 70 GeV and at 19.2 GeV; deviations are observed for $p/p_{max} \leq .6$.

E_0 (GeV)	P (GeV/c)	(Θ) (mrad)	K^-/π^- (10^{-2})	$\bar{p}/\pi^-$ (10^{-3})
20.1	11.4	12	1.7 ± 0.1	0.53 ± 0.07
43.1	24.6	0	2.6 ± 0.1	2.1 ± 0.1
	30.7	0	0.89 ± 0.03	0.28 ± 0.02
	40.5	0	3.1 ± 0.1	2.50 ± 0.15
	40.1	12	3.4 ± 0.1	2.90 ± 0.15
	45.3	5	2.4 ± 0.1	1.31 ± 0.07
	45.3	15	2.1 ± 0.1	1.46 ± 0.07
	47.0	3	1.8 ± 0.2	1.10 ± 0.10
70.0	50.0	0	1.15 ± 0.06	0.49 ± 0.03
	50.0	8		
	50.1	10	1.11 ± 0.06	0.50 ± 0.03
	55.0	4	0.36 ± 0.03	0.09 ± 0.01
	60.0	0	0.080 ± 0.006	0.011 ± 0.003
	60.0	3		
	60.0	5		
	63.0	2		
	63.0	6		
	66.0	0		
	66.0	4		
	69.0	2		
	69.0	4		

Table V - Particle ratios and π^- production cross-sections as a function of secondary momentum (P) and production angle (θ) for several incident proton energies E, (lab. system) (From Ref. 29).

References and Notes to Chapter 2

1. Serpukhov-Cern collaboration, Phys. Letters **30B**, 500 (1969) and paper presented at the Kiev Conference (1970).
2. Since the Serpukhov data (Ref. 1) on total cross sections for negatively charged particles on proton and deuterium, many theoretical papers have appeared commenting, on the one hand, on the various mechanisms by which one could explain the apparent violation of asymptotic theorems and, on the other hand, on the implications of the possible violation of such theorems. A discussion on these points is, clearly, outside the scope of the present survey.
3. T. Hofmokl and A. Wroblenski, Phys. Letters **31B**, 391 (1970).
4. In this Section we denote by a,, the topological cross section for production of 2k charged particles. In the following, the notation a,: will also be used to denote the single production reaction for creation of n particles (charged or not) in the final state.
5. D. B. Smith, R. J. Sprafka and J. A. Anderson, Phys. Rev. Letters 23, 1064 (1969).
6. Almeida *et al.*, Phys. Rev. 174,1638 (1968); Holmgsen *et al.*, Nuovo Cimento **57A**, 20 (1968); Bodini *et al.*, Nuovo Cimento **57A**, 475 (1968); Alexander *et al.*, Phys. Rev. *154*, 1284 (1967); Eisner *et al.*, Phys. Rev. **138B**, 670 (1965); Hart *et al.*, Phys. Rev. 125, 747 (1962); Pickup *et al.*, Phys. Rev. *125,* 2091 (1962); Yekutieli *et* al., Nuc. Phys. **B18,** 305 (1970).

7. A. Wroblenski, Phys. Letters **32B**, 145 (1970).
8. W. E. Ellis *et al.*, BNL 13544 (1970).
9. Connolly *et al.*, BNL 13694 (1970).
10. See for instance E. Fermi., Prog. Theor. Phys. 5, 570 (1950); for a complete review, see Hagedorn *et al.*, "Atlas of...", Cern preprint (1970).
11. D. Amati, S. Fubini and A. Stanghellini, Nuovo Cimento **26,** 896 (1962) and L. Bertocchi, S. Fubini and M. Tonin, Nuovo Cimento 25, 626 (1962).
12. G. F. Chew and R. Pignotti, Phys. Rev. 176,2112 (1968).
13. See, for instance, Y. Pal and B. Peters, Mat. Fys. Medd. Dan. Vid. Selks. **33,** 3 (1964).
14. C. B. A. McCusker and L. S. Peak, Nuovo Cimento 31, 525 (1964).
15. S. Yamada and M. Koshiba, Phys. Rev. 157, 1279 (1967).
16. L. W. Jones *et al.*, UM *HE* 70-15 (1970).
17. Actually, in Eq. (2.16) the coniribution of σ_2 has been neglected both in the numerator as well as in the denominator. As a single contribution is expected to be negligible as compared to the sum of all the others, this should not alter considerabl- the result. As a correction in Eq. (2.16), one gets

$$\langle n_c \rangle \simeq 6 - 4\sigma_2 / \sum_{k=2}^{\infty} \sigma_{2k} \lesssim 6.$$

18. It may also happen, of course, that none of the models previously mentioned give a fair description of the actual phenomena and that the structure of the dynamics of strong interactions at high energies will still be different.
19. S. Brandt, paper 775 presented at the 1968 Vienna Conference.
20. *C.* P. Wang, Phys. Rev. 180, 1463 (1969).
21. Proceedings of the "Colloquiiim on High Multiplicity Hadronic Interactions": École Polytechnique, Paris (1970); see review paper by A. Wroblenski.
22. D. Horn and D. Silver, Phys. Rev. **D2,** 2082 (1970).
23. For a different approach to the same problem see **Ch.** 4, Sec. e (to appear in **Part II** of this survey).
24. G. Kaiser, Cambridge preprint HEP 70-8 (1970).
25. A. Martin, Nuovo Cimento **29,** 993 (1963).
26. J. L. Day *et al.*, Phys. Rev. Letters **23,** 1055 (1969).
27. R. Panvini, BNL 14126 (see also Ref. 5 of the literature quoted in this paper).
28. F. Turkot, Proceedings of the "Topical Conference of High Energy Collisions of Hadrons", Cern (1968).
29. Serpukhov-Cern Collaboration, Phys. Letters **29B**, 48 (1969).
30. J. A. Allaby *et al.*, paper presented at the 14th International Conference on High Energy Physics; Vienna 1968 (Geneva 1968).

3. Recent Developments in the Study of the Phase Space

3.1 Introduction

A collision with n particles in the final state

$$A + B \rightarrow 1 + 2 + \ldots + n \tag{3-1}$$

is characterized by $3n$ variables associated with the momenta of the final state particles. The energy-momentum conservation reduces to $3n - 4$ the number of independent variables. As n increases, the kinematical situation becomes thus extremely involved due to the large number of variables that one has to consider.

For a uniform distribution of evenis, i.e., in the absence of dynamics, process (3-1) is described by the phase space 4,. In faci, if there is no dynamical mechanism at work. the transition probability $dP_{,}$ of reaciion (3-1) is simply proportional to the corresponding volume element of the relativistically invariant phase space given by

$$d\phi_n = \prod_{i=1}^{n} \frac{d^3 p_i}{2E_i} \delta^3 \Big(\sum_{i=1}^{n} \mathbf{p}_i - \mathbf{p}_A - \mathbf{p}_B \Big) \delta \Big(\sum_{i=1}^{n} E_i - E_A - E_B \Big). \tag{3.2}$$

The full transition probability

$$dP_n = |M|^2 \, d\phi_n \tag{3-3}$$

deviates from the phase space because of the matrix element modulus $|M|^2$ where all the dynamics is concentrated.

In the following, we shall have to consider the properties of the phase space on the one hand and the various theoretical models suggested to describe $|M|^2$ on the other hand. The first problem will be briefly considered in the present chapter whereas the discussion of $|M|^2$ will represent the main subject to be discussed in Part II.

The correlation between the kinematics and the dynamics of a given process will consist in expressing both in terms of the same set of variables conveniently chosen so as to furnish information on the possible dynamical structure of the process itself.

For this reason, we prefer, in the following of this chapter, to concentrate on some of the most general properties of the phase space rather than entering in details into the lengthy calculations which are customary when treating this subject. These formal developments, in fact, while available in the many review papers existing in the literature', would unnecessarily obscure the physical situation.

Thus, we will consider here first of all the problem of the energy dependence of the phase space. This will allow us to subtract from the experimental cross sections their kinematical energy dependence. Secondly, we shall discuss some of the representations used to describe the phase space choosing those that are more useful for their dynamical implications, i.e., those that are more likely to give us the clue to read the dynamics of the distributions of events.

3.2 Energy Dependence of the Phase Space

In the *c.m.* system, the phase space integral that gives the energy dependente of reaction (3.1) in the absence of dynamics, takes the form

$$\phi_n = \int \cdots \int \prod_{j=1}^{n} \frac{d^3 P_j}{2E_j} \delta^3 \left(\sum_{j=1}^{n} \mathbf{P}_j\right) \delta\left(\sum_{j=1}^{n} E_j - E_{c.m.}\right) \tag{3-4}$$

where $E_{c.m.}$ = E, + E,. For given values of the masses m_j of the outgoing particles, ϕ_n is function of E,,,, only.

It is found' that, at threshold where $E^2_{c.m.} \simeq m_1'^2 + m_2'^2$ (m_1', m_2' being the masses of the incoming particles) one has

$$\phi_n \simeq \left(E_{c.m.} - \sum_{j=1}^{n} m_j\right)^{(3n-5)/2} \tag{3-5}$$

whereas, at high energies

$$\phi_n \simeq E_{c.m.}^{2n-4}\,. \tag{3-6}$$

We remember that the invariant form of the phase space integrals can be written in terms of recurrence relations between the integrals of spaces of different dimensions. This is very useful in order to simplify the explicit calculations.

We notice that the energy dependence of the phase space integrals grows as a power of $E_{c.m.}$ which increases with the number of particles in the final state. The rate of decrease to such a behavior of the cross sections obtained by dividing by the flux of the incoming particle F is only a factor of $E^2_{c.m.}$. Thus, in the high energy limit,

$$\frac{\phi_n}{F} \simeq E_{c.m.}^{2n-6}\,. \tag{3-7}$$

3.3 Representations of the Phase Space

The $3n-4$ independent momenta variables can be used to construct new sets of Lorentz'invariant variables by forming scalar products of four-momenta or linear combinations of them[2]. This set of variables, however, does not seem very useful for making comparisons with the experiments[3]. From this point of view, other representations are more convenient which, together with relativistically invariant variables, introduce angular variables[4] (see also P. Nyborg, Ref. 1).

Among the representations of the latter kind, we will discuss in the following:

a) the Muirhead triangular representation and

b) the Van Hove longitudinal phase space representation.

3.3a The Muirhead Triangular Representation

This representation has been suggested[5] to describe reactions of the form

$$A + B \to 1 + 2 + 3. \tag{3-8}$$

We calculate the four-momentum transfer for each emitted particle (1, 2, 3) with respect to the same initial particle (say A). The three variables thus defined t_{A_1}, t_{A_2}, t_{A_3}, at high energy are not independent:

$$t_{A_1} + t_{A_2} + t_{A_3} \simeq \text{const.} \tag{3-9}$$

Thus, if we plot graphically these three variables on axes mutually inclined of 120°, the figure that obtains is a triangle (see Fig. 16).

The representation generalizes easily. For

$$A + B \to 1 + 2 + 3 + 4, \tag{3-10}$$

we have a tetrahedron: for

$$A + B \to 1 + 2 + \ldots + n, \tag{3-11}$$

one has a regular simplex at $(n-1)$ dimensions.

In this representation, the density of points coming from the pure phase space (Fig. 16) is practically uniform in the triangle in the limit of very high energy.

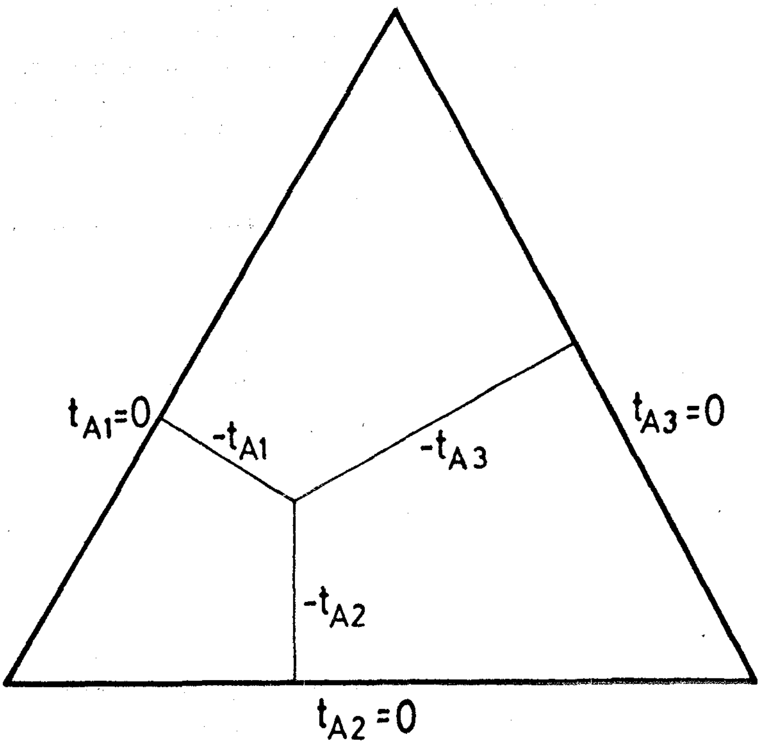

$A+B \longrightarrow 1+2+3$

$t_{A1}+t_{A2}+t_{A3}=\mathbf{Const.}$

Fig. 16 - The Muirhead plot.

3.3b The Van Hove Longitudinal Phase Space Representation

We shall discuss now in some detail this representation because we believe that it is the one which is more likely to incorporate already important dynamical properties of high multiplicity hadronic interactions.

The basic observation here (which plays the role of Eq. (3-9) in the case of the Muirhead representation) is the experimental fact that, at high energies, the transverse component of the momenta in the final state are usually small and independent of the incident energy (see Sec. 2.6).

The idea is then of separating the phase space in its longitudinal and transverse components. There follows that, with increasing energy, the phase space dilatates in its longitudinal component only.

The Van Hove representation stems from the possibility of shówing that for a collision with n final particles, the distribution of the phase space reduces to an (n – 2)-dimensional manifold.

Consider reaction (3-1). Let $E_{c.m.}$ be the total *c.m.* energy, $p_{L,i}$ and $p_{T,i}$ the longitudinal and transverse momenta of the i-th final particle and $E_{c.m.i}$ the energy of this particle in the *c.m.* system.

We notice that

$$E_{c.m.i} = (m_i^2 + p_{T.i}^2 + p_{L,i}^2)^{1/2} = (m_i'^2 + p_{L,i}^2)^{1/2} \tag{3-12}$$

where $m_i'^2 = m_i^2 + p_{T.i}^2$ is the effective (squared) mass for the longitudinal motion. In the *c.m.* system, the energy-momentum conservation demands

$$\sum_{i=1}^{n} E_{c.m.i} = E_{c.m.}, \tag{3-13}$$

$$\sum_{i=1}^{n} p_{L,i} = 0, \tag{3-14}$$

$$\sum_{i=1}^{n} p_{T,i} = 0. \tag{3-15}$$

The suggestion in Ref. 6 is now of representing each individual collision by the point $(p_{L,1}, p_{L,2}, \dots p_{L,n})$ in the n-dimensional Euclidean space S_n. On the other hand, all these points must lie on the (n – 1)-dimensional hyperplane $L_{(n-1)}$ defined by Eq. (3-14). $L_{(n-1)}$ is the longitudinal phase space.

For given values of $p_{T,i}$, and therefore of m_i', the point of coordinate $(p_{L,1}, \dots p_{L,n})$ lies on the hypersurface $K_{(n-2)}$ defined in $L_{(n-1)}$ by the equation

$$\sum_{i=1}^{n} (m_i'^2 + p_{L,i}^2)^{1/2} = E_{c.m.}. \tag{3-16}$$

If $p_{L,i}^2 \gg m_i'^2$ (high energy limit), Eq. (3-16) which defines the hypersurface $K_{(n-2)}$ becomes

$$\sum_{i=1}^{n} |p_{L,i}| = E_{c.m.}, \qquad (3\text{-}17)$$

which identifies in $L_{(n-1)}$ a polyhedron $H_{(n-2)}$.

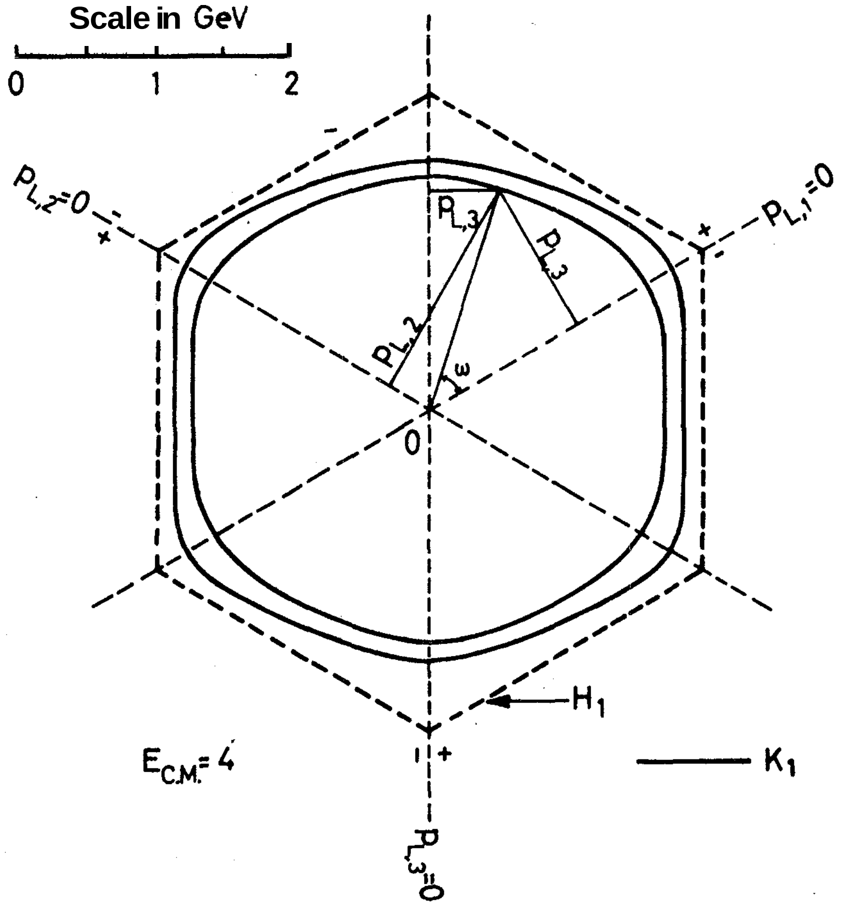

Fig. 17 - The longitudinal phase space plot (Van Hove) for $n = 3$ at E,,,, = 4 GeV.

Fig. 17 shows an example of the longitudinal phase space for the case of a final state $\pi\pi N$ and E,,,, $= 4\, GeV$. Since **n** = **3,** the longitudinal phase space L, is two dimensional and contains the polyhedron H, which is a regular hexagon. The curve K_1 is given for two different sets of values of $(|p_{T,1}|, |p_{T,2}|, |p_{T,3}|)$ and, more precisely, (inner curve) for **(0.4, 0.4,** 0.5) and (outer curve) for (0, **0,** O). The masses are $m_1 = m, = m_\pi = .14$ and $m_3 = m_N = .94$ (c = 1 and all quantities in GeV).

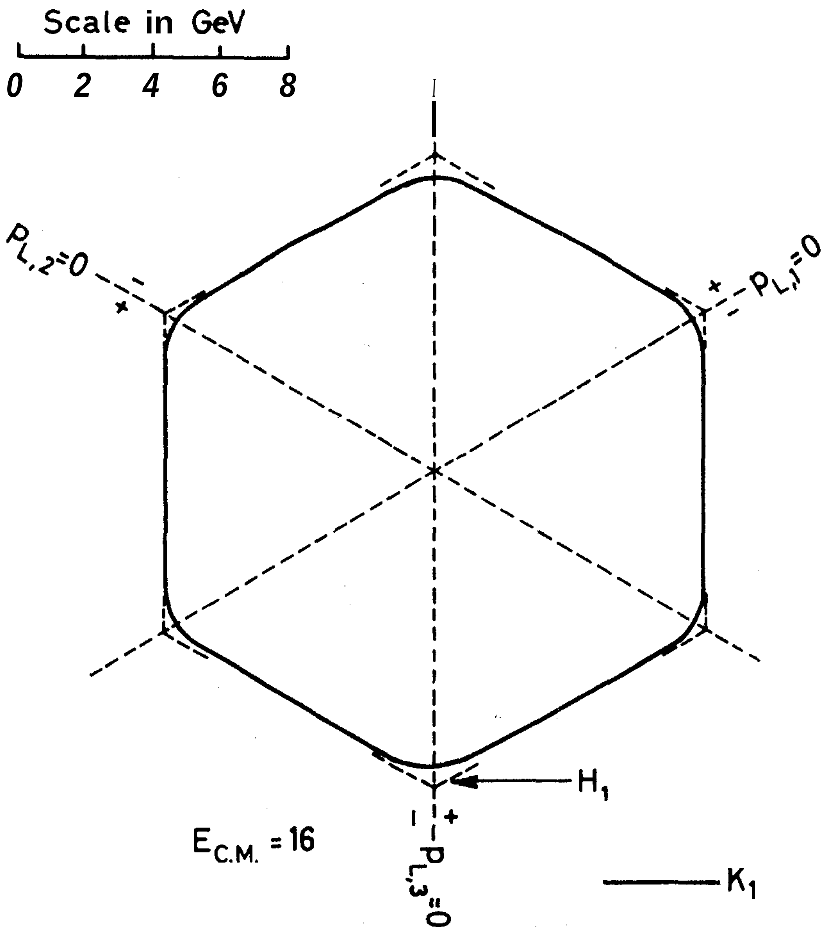

Fig. 18 - The longitudinal phase space plot (Van Hove) for $n = 3$ at E,, = 16 GeV

The use of polar coordinates (p_L, w) in the plane L_3 allows one to give the parametric expression for the point $(p_{L,i})$ as

$$p_{L,1} = (2/3)^{1/2}\, p_L \sin w$$

$$p_{L,2} = (2/3)^{1/2}\, p_L \{-(1/2)\sin w - (\sqrt{3}/2)\cos w\}$$

$$p_{L,3} = (2/3)^{1/2}\, p_L \{-(1/2)\sin w + (\sqrt{3}/2)\cos w\}, \tag{3-19}$$

where the scale factor is $(2/3)^{1/2}$ and

$$p_L = (p^2_{L,1} + p^2_{L,2} + p^2_{L,3})^{1/2}.$$

Fig. 18 shows the case for $p_{c.m.} = 16$ (all the other parameters are as in Fig. 17).

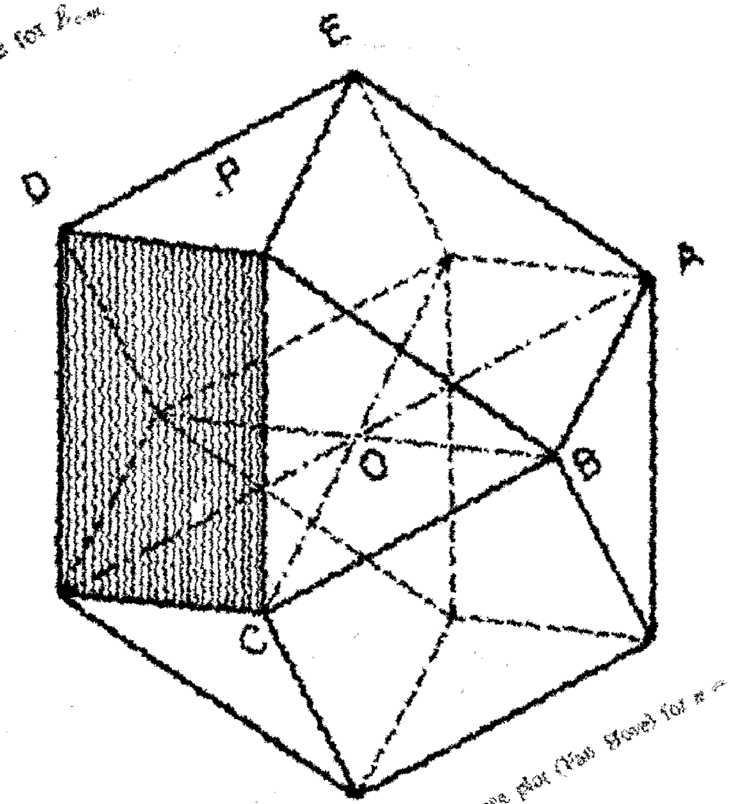

Fig. 19 - The longitudinal phase space plot (Van Hove) for $n = 4$.

When there are four particles in the final state ($n = 4$), the longitudinal phase space L, is three dimensional and the polyhedron H_2 defined in it (a cubeoctahedron) is given in Fig. 19. In the space S_4 of points $(p_{L,1}, \dots p_{L,4})$, the $p_{L,i}$ are the distances of the points of the polyhedron from the planes AOB, OBD, OCE, OAE; the scale factor is $(3/4)^{1/2}$ (whereas in the n-dimensional case it would be $(n-1)^{1/2} n^{1/2}$).

References to Chapter 3.

1. For a complete treatment of the phase space see, for instance: R. Hagedorn, *Relativistic Kinematics*, Benjamin, New York (1964). O. Skieggestad, Cern Easter School (1964) Vol. II, Cern preprint 64-13 (1964). J. Bartke, Proceedings of the Hercegnovi Summer School (1970). P. Nyborg, Proceedings of the Hercegnovi Summer School (1970). V. A. Kolkunov, Soviet JETP 16,1025 (1963). V. A. Kolkunov, N. N. Meiman and E. S. Nikolaevskii, Soviet JETP 9, 316 (1969).
2. V. E. Asribekov, Soviet JEPT 15, 394 (1962).
3. E. kycking and K. Kajantie, Phys. Rev. 187, 2008 (1969).
4. A. Krzywicki, Proceedings of the Colloquium on High Multiplicity Hadronic Interactions, Paris (1970).
5. See D. R. O. Morrison, Proceedings of the Lund International Conference on Elementary Particles (1968).
6. L. Van Hove, Phys. Letters **28B**, 429 (1969) and Nucl. Physics **B9,** 331 (1969).